Colloid & Polymer Science Colloid Polym Sci 272:504–515 (1994)

Elastomeric properties of end-linked networks of high cross-link functionality. Accounting for possible changes in effective functionality with extent of reaction and chain-length distribution

M. A. Sharaf*), J. E. Mark, and E. Ahmed[1])

Department of Chemistry and Polymer Research Center, The University of Cincinnati, Cincinnati, Ohio, USA
[1]) Department of Mathematics, United Arab Emirates University

Abstract: This study reanalyzes some elastomeric properties in elongation reported for poly(dimethylsiloxane) (PDMS) networks of high cross-link functionality which had been prepared by using multifunctional siloxane oligomers to end link vinyl-terminated PDMS chains. The extent of reaction of the vinyl end groups P_{vi} spanned the range of 0.40 to 0.95. These networks had elongation moduli that significantly exceeded the values predicted by the Flory–Erman theory, except at very low values of P_{vi}. Trends in their stress-strain isotherms, as characterized by the Mooney–Rivlin constants $2C_2$ and the ratio $2C_2/C_1$, also appeared to be different from those predicted by theory. Neglected in such standard analyses, however, was the fact that the segments between cross-links along the junction precursor molecules can themselves act as short network chains, contributing to the modulus and giving a strongly bimodal distribution of both network chain lengths and cross-link functionalities. Of particular interest is the apparent change in functionality with extent of reaction and chain length distribution. The results thus obtained do suggest strong dependence of the observed values of the phantom modulus on the network chain-length distribution, particularly at very small values of the ratio of the length of the short chains to the long ones. Calculations based on recognition of these complications can be used to characterize more realistically the deformation of such networks. The results give much better agreement with experiment. Such behavior could be an important characteristic of elastomeric networks in general.

Also, a preliminary attempt was made to bridge theory with experiment based on Kloczkowski, Mark, and Erman's recent theory of fluctuations of junctions in regular bimodal networks. The agreement between theory and experiment thus obtained is rather satisfactory and lends further support to assumptions that take into account the possibly bimodal nature of these high-functionality networks.

Key words: Model networks – bimodal networks – poly(dimethylsiloxane) – elastomers – rubber elasticity – mechanical properties – elongation modulus – stress-strain isotherms – end-linking reactions – Flory–Erman theory

Introduction

Polysiloxane networks of high junction functionality ϕ can be prepared by end linking α,ω-divinyl poly(dimethylsiloxane) (PDMS) using the reactive Si-H groups in poly(hydromethylsiloxane) $[-SiH(CH_3)O-]_x$. Each hydrogen atom on one of these silicon atoms can potentially add to

*) Present Address: Department of Chemistry, United Arab Emirates University, P.O. Box 17551, Al Ain, United Arab Emirates; on leave from Cairo University at Beni-Suef, Beni-Suef, Egypt.

one of the vinyl end groups. Such networks have been prepared and their elastomeric properties reported in the literature [1–7]. They have been formed using various stoichiometries, specifically differing values of the molar ratio r of Si-H groups to vinyl end groups. Networks with high extents of vinyl group reaction ($P_{vi} > 0.9$) were prepared by having r slightly greater than unity (i. e., excess Si-H groups). One of these studies [6] dealt with high-functionality networks formed such that P_{vi} covered a wide range of values, from 0.40 to 0.95. This was achieved by having $r < 1$, under which conditions the end-linking reaction does not go to completion.

It is possible to use the recent molecular theory of Flory and Erman [8–12] to interpret and even predict the properties of such high-functionality networks, particularly with regard to several important results. The most interesting of these is the observation that the small-strain and large-strain moduli exceeded the values predicted from the expected junction functionality ϕ and the junction concentration [1–7]. Another interesting observation pertains to the effect of junction functionality on the magnitude of the junction fluctuations. According to the Flory–Erman theory [8–12], junctions of high functionality are severely entangled by neighboring chains, and this makes their displacement under deformation very nearly affine (linear) in the strain. This should greatly affect the empirical Mooney–Rivlin $2C_2$ constant (which represents the decrease in modulus resulting from the deformation becoming progressively non-affine with increased elongation). Specifically, the chain-junction entangling prevents the deformation from becoming non-affine, and thus $2C_2$ is predicted to be very small (asymptotically approaching zero with increase in ϕ). The reported values of $2C_2$, however, were relatively large, even for $\phi > 30$ [1–7].

In most of these studies [2–6], attention was focused only on the small-strain modulus, where the deformation is most likely to be near the affine limit. The increases in the small-strain modulus over the values predicted by theory for such networks were attributed to contributions from inter-chain (trapped) entanglements [2–6]. Recently, however, the present authors [12–14] suggested an alternative interpretation which focuses on the short chain segments between the cross-linking points along the junction precursor molecules. It was suggested that such segments can act as short network chains, thus contributing to the modulus and giving strongly bimodal distributions of network chain lengths. The unusual connectivity of such short chains to the rest of the network can possibly give a bimodal distribution of cross-link functionalities as well [12–14]. Re-examination of some of the published results on such networks in which the extent of reaction P_{vi} was high, greater than 0.9, gave much better agreement between experiment and theory [13]. More specifically, consideration of the possibly bimodal nature of these high-functionality networks provided a reasonable explanation of their unexpectedly high values of the modulus [12, 13]. This revised interpretation also explained the observations that the empirical constant $2C_2$ was not as small as expected. The expected suppression of junction fluctuations by the large amounts of entangling around the high-functionality junctions was apparently offset by decrease in entangling resulting from the low functionality of the junctions to which these short chains are attached, and because of the reduced interpenetration associated with short chains in general [8–10].

Additional complications in such networks are possible changes in the effective cross-link funtionality with elongation. At low extents of reaction, an end-linking molecule would have only some of its Si-H groups reacted and could act as a sequence of trifunctional junctions at low deformation. At high extents of reaction, however, these segments would be very short and could be stretched out sufficiently at high elongations to make the end-linking molecule act as a single high-functionality junction. Thus, the effective functionality could depend on extent of deformation as well as extent of reaction.

There is thus particular interest in the particular experimental study (6) in which networks were intentionally prepared so as to cover a wide range of extent of reaction, specifically $P_{vi} \sim 0.40$–0.95. The extent of reaction should affect the numbers and lengths of the short chains introduced from the end-linking molecules, and also the effective functionalities they impose on junctions to which the long chains are connected. The present investigation therefore re-examines these experimental results, in a manner accounting for these additional possible complications.

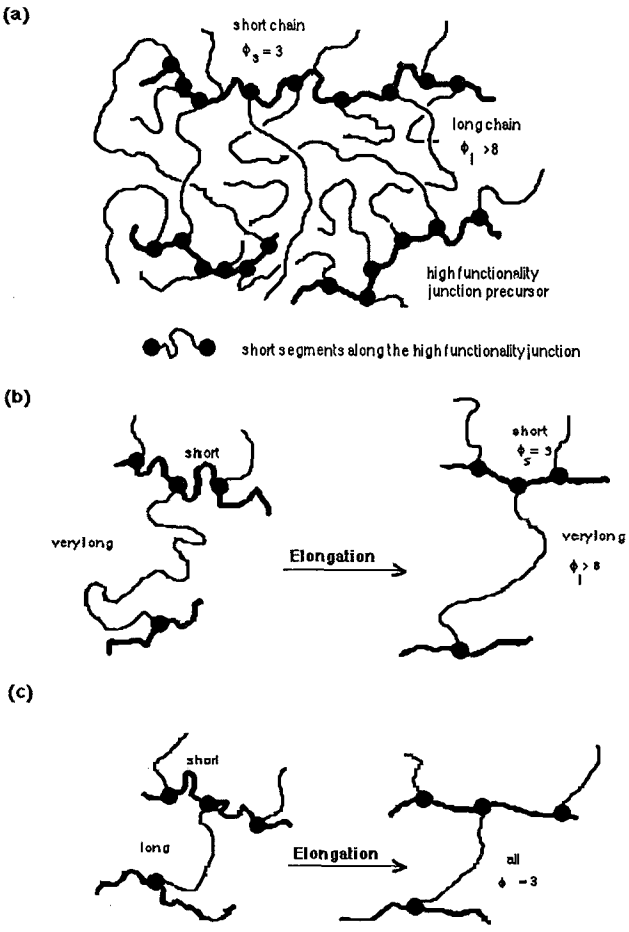

Fig. 1. Sketches showing parts of a high-functionality network in the undeformed state and in elongation. Portion (a) shows the undeformed network, with chains coming from the long vinyl-terminated polymer shown as thin lines, and the short chains coming from segments of the end-linking molecules as thick lines. In all the sketches the dots represent cross links and the functionality ϕ_S sensed by the short chains is always three. Portion (b) illustrates the effect of elongation on the junction functionality ϕ_L sensed by the long chains in the case of very high extents of reaction. The stretching out of the very short chains makes the entire end-linking molecule now act as one junction of very high functionality. Sketch (c) shows the absence of such a change in ϕ_L in the case of lower extents of reaction. The chains contributed by the end-linking molecule are now insufficiently short for the end-linking molecule to act as anything other than a series of trifunctional junctions, even at high elongations

Structural considerations

Some of the largest improvements in properties of networks intentionally made to be bimodal occur when the short chains consist of only about a half-dozen skeletal bonds, and the lengths for maximum effect could even be smaller [12–17]. Such short chains would in effect always be attached to trifunctional junctions ($\phi_s = 3$), as is illustrated in part (a) of Fig. 1. As was pointed out previously, 2ν of these short chains would be generated by the ν long chains present in the network [12, 13]. The long chains would also sense the junctions at their ends to be trifunctional ($\phi_L = 3$), except in the case of high extents of reaction and high elongations. Under these conditions, illustrated in part (b) of Fig. 1, the chains coming from the end-linking molecules would be so short that the high elongations would extend them to the point that the end-linking molecule would act as a single junction of high functionality. At lower extents of reaction, illustrated in part (c), these chains would probably not be short enough for this to occur.

Elasticity equations

For any type of elastomeric network, the reduced stress or modulus in elongation is defined by (10)

$$[f^*] = f\upsilon_2^{1/3}/[A^*(\alpha - \alpha^{-2})] \,. \tag{1}$$

In these equations, f is the equilibrium value of the force, A^* the undeformed cross sectional area, α the relative length (elongation) of the sample, and υ_2 the volume fraction of polymer during the stress-strain measurements.

For an affine deformation, the modulus is given by the relationship [8–10]

$$[f^*]_{\text{aff}} = \nu RT\upsilon_{2C}^{2/3} \,, \tag{2}$$

where ν is the number density of elastically-effective chains, R the gas constant, T the absolute temperature, and υ_{2C} the volume fraction of polymer chains in the system being cross-linked that were successfully incorporated in the network structure.

In this connection, it is essential to note here that the identification of the effective chain density ν (relevant to rubber elasticity theory) with the active chain density ν_a is an approximation that should be proper for the networks of high functionality being considered [22].

In the phantom network, which is approached experimentally at high elongations, the chains are assumed to be devoid of material properties, i. e., that they can move freely through one another [8–10, 18–22]. The mean positions of the junctions are affine in the strain, but the fluctuations about the mean positions are invariant with strain. The modulus is given by [8–10, 8–22]

$$[f^*]_{ph} = \xi RT\upsilon_{2C}^{2/3} , \tag{3}$$

where [18–22]

$$\xi = \nu_a - \mu_a = \nu - \mu \tag{4}$$

is the cycle rank of the network, μ_a is the number density of the elastically-active junctions, and ν and μ are the number density of elastically-effective chains and junctions, respectively. For a perfect network having functionally ϕ, the cycle rank is expressed as [18–22]

$$\xi = \left(1 - \frac{2}{\phi}\right)\nu_a \tag{5}$$

where the front factor would be $A_\phi = \left(1 - \frac{2}{\phi}\right)$. Finally, in a perfect network, the number of active junctions μ_a is given by [18–22]

$$\mu = \mu_a = (2/\phi)\nu_a = [2/(\phi - 2)]\xi . \tag{6}$$

Therefore, values of the phantom modulus are based only on contributions from active chemical (covalent) crosslinks.

The role of connectivity in the phantom network is of great importance. As discussed by Graessley [18–21], the cycle rank of a network is the number of cuts required to reduce it to a spanning tree (free of cyclics). This would mean that the cycle rank depends only on the number of active chains ν_a and the junction functionality ϕ, and is totally independent of the chain-length distribution. It is to be noted here that Graessley later modified this expression to [21]

$$\xi = \nu_a - h\mu_a = (1 - 2h/\phi)\nu_a , \tag{7}$$

(with h being an adjustable parameter between 0 and 1) to take into account trapped interchain entanglements. A consequence of this equation is that the phantom modulus would have values different from those predicted by the density of the chemical crosslinks. In other words, this equation yields values of the front factor $(1 - 2h/\phi)$ that are generally higher than the value $(1 - 2/\phi)$ for an idealized phantom network.

These equations can be directly applied to the high-functionality networks in the most complicated case: high elongations of networks which have very short chains by virtue of their high extents of reaction. As already described, they could now have bimodal distributions of cross-link functionality, as well as of network chain lengths. If the short chains are considered to be elastically effective and their connectivity to the long ones is taken into account, the modulus in the phantom limit would then be [12–14]

$$\begin{aligned}[f^*]_{ph} &= [f^*]_L + [f^*]_S = (\nu_a - \mu_a)RT \\ &\quad + (1 - 2/\phi_S)2\nu_a RT \\ &= (\nu_a - \mu_a)RT\upsilon_{2C}^{2/3} + (2/3)\nu_a RT\upsilon_{2C}^{2/3} . \end{aligned} \tag{8}$$

It is obvious that the functionality ϕ_S associated with the short chains (S) is always three. The average functionality ϕ_L associated with the long chains (L) is presumably 8 or larger [1–7]. In any case, in the limit of very high functionality the number of elastically-active junctions would be very small. Consequently, one obtains [12–14]

$$[f^*]_{ph} = (5/3)\nu_a RT\upsilon_{2C}^{2/3} . \tag{9}$$

The effective value of $[f^*]_{ph}$ is thus larger than what would be expected from network topological considerations alone [8–13, 18–22]. Consequently, this result is at variance with considerations discussed above which require preservation of the cycle rank regardless of the network chain-length distribution or any changes in the effective functionality of the long network chains. However, this expected invariance is in disagreement with a great deal of experimental evidence. The relevant experiments have shown that the elastomeric properties for bimodal networks *are* dependent on the mole fraction of the short chains present in the network as well as the ratio of lengths of the short chains to the long ones [12–17]. More specifically, bimodal networks can have moduli significantly larger than those having unimodal distributions with the same average molecular weights between junctions.

In the treatments ignoring the presence of the short chains and their connectivity to the long

ones, the phantom modulus in the limit of high extent of reaction would simply be [1–7, 11]

$$[f^*]_{ph} = (\nu_a - \mu_a)RT \approx \nu_a RT \upsilon_{2C}^{2/3} . \quad (10)$$

At low extents of reaction, the situation would be different in that all junctions would be effectively trifunctional. The modulus in the phantom limit would then be

$$[f^*] = (1/3)3\nu RT \upsilon_{2C}^{2/3} = \nu RT \upsilon_{2C}^{2/3} . \quad (11)$$

This means that the increase in the modulus from the increased number of chains is exactly offset by the decrease in functionality, and the result is the same as that obtained by treating the network as a simple unimodal network with high functionality. These ideas concerning cross-link functionality in bimodal networks are considered more quantitatively elsewhere [23, 24].

Comparisons between experiment and the revised theory

The experimental results analyzed are for high-functionality PDMS networks formed in the undiluted state and having extents of reaction $0.40 < P_{vi} < 0.95$ (6). The results thus obtained are summarized in Table 1. The number of elastically-active chains and other structural parameters of the network were determined from P_{vi}, the fraction ω_s of extractable sol, and number-average molecular weight M_n of the α, ω-divinyl PDMS using relationships presented elsewhere [2–6]. All the networks had $\phi_0 = 43.9$ (6). The effective functionality ϕ_L is given by [6, 11]

$$\phi_L = \phi_0 P_{vi}^2 / r , \quad (12)$$

where ϕ_0 is the (maximum) functionality of the end-linking molecule, and r the molar ratio of the SiH groups to the vinyl end groups. The number of junctions μ_a would be given by [3]

$$\mu_a = (2/\phi_L)\nu_a . \quad (13)$$

Neglected in analyses based on branching theory is the fact that such large numbers of network imperfections generated by the incompleteness of end-linking would act as diluent, even in the dry (unswollen) state [27]. As shown in Eq. (1), the defining relationship for $[f^*]_{ph}$ should include the factor $\upsilon_2^{-1/3}$, taking this into account, where υ_2 is the volume fraction of elastically-active chains in the network (as calculated from branching theory [3]). Hence, values of $[f^*]_{ph}$ predicted by Eq. (4) would be

$$[f^*] = \xi RT \upsilon_{2C}^{2/3} \upsilon_2^{-1/3} . \quad (14)$$

The reported experimental values of $[f^*]_{ph}$ had been calculated without the factor $\upsilon_2^{-1/3}$ described above. Effects of network imperfections on the elastomeric properties are discussed in greater detail elsewhere [28].

The quantity of primary interest in this treatment is the reduced force $[f^*]$ given by Eq. (1) in the limit $\alpha \to \infty$. For this purpose the Mooney–Rivlin representation [25, 26]

$$[f^*] = 2C_1 + 2C_2\alpha^{-1} \quad (15)$$

will be employed, with $2C_1$ approximating the reduced force in the limit $\alpha \to \infty$. According to theory, this constant may be approximately identified with the reduced force $[f^*]_{ph}$ [8–17]. Although values of $2C_1$ thus obtained slightly overestimate values of $[f^*]_{pd}$ due to difficulties in the linear extrapolations to $\alpha \to \infty$, the results should be suitable for the present purposes. The other constant $2C_2$ is ascribed to enhancement of the phantom modulus $[f^*]_{ph}$ at small strains from constraints imposed on the junction fluctuations by neighboring network chains. In other words, it is a measure of the departure of the relationships obtained from those of the phantom network theory [8–10, 22].

Figure 2 presents values of $2C_1$ for all data points [6] (with different effective functionalities) as a function of $\nu_a RT \approx \nu RT$. The dashed line represents previous calculations based on Eq. (10) for a unimodal network with only the long chains taken into account. The solid line represents calculations of $[f^*]_{ph}$ based on the present approach, which does take into account the short chains contributed by the end-linking molecules, according to Eq. (8). Excellent agreement between theory and experiment is seen to occur between the two bounds of this revised model (set by Eqs. (8) and (11)), when the bimodal nature of these high-functionality networks is taken into consideration.

In a similar manner, the revised interpretation can explain reported values of $2C_2$ (and the more relevant ratio $2C_2/2C_1$) not being as small as

Table 1. Elastomeric properties of high-functionality polydimethylsiloxane (PDMS) Networks[a])

M_n g mol^{-1}	M_n(S) g mol^{-1}	γ[c])	r	ω_s	P	ϕ_0	ϕ_e	v_2[d])	vRT N mm^{-2}	$[f^*]_u$[e]) N mm^{-2}	$2C_1$ N mm^{-2}	$[f^*]_b$[f]) N mm^{-2}	$2C_2$ N mm^{-2}	$2C_2/2C_1$	$2C_1/vRT$[g])
9320	81	0.000	1.205	0.0000	0.970	43.9	34.3	0.900	0.243	0.229	0.435	0.391	0.098	0.225	1.79
	84	0.009	1.121	0.0063	0.920	43.9	33.1	0.855	0.226	0.212	0.357	0.363	0.073	0.204	1.58
	111	0.012	0.979	0.0623	0.749	43.9	25.1	0.629	0.160	0.147	0.168	0.253	0.356	2.119	1.05
	109	0.012	0.954	0.0637	0.746	43.9	25.6	0.626	0.159	0.146	0.154	0.252	0.068	0.442	0.97
	116	0.012	0.927	0.0822	0.711	43.9	24.0	0.595	0.145	0.133	0.162	0.229	0.032	0.198	1.12
	151	0.016	0.864	0.1560	0.603	43.9	18.5	0.527	0.102	0.091	0.129	0.160	0.000	0.000	1.26
11100	88	0.008	1.201	0.0046	0.932	43.9	31.7	0.874	0.193	0.181	0.316	0.310	0.053	0.168	1.63
	135	0.012	1.106	0.0768	0.721	43.9	20.6	0.603	0.125	0.113	0.143	0.196	0.041	0.287	1.14
	163	0.015	1.006	0.1390	0.625	43.9	17.0	0.537	0.093	0.082	0.109	0.144	0.000	0.000	1.17
	168	0.015	0.980	0.1520	0.608	43.9	16.6	0.529	0.088	0.077	0.102	0.136	0.000	0.000	1.16
	173	0.016	0.959	0.1640	0.593	43.9	16.1	0.522	0.083	0.073	0.080	0.128	0.000	0.000	0.96
	206	0.019	0.920	0.2160	0.533	43.9	13.5	0.507	0.065	0.055	0.074	0.099	0.005	0.068	1.14
17400	122	0.007	1.652	0.0052	0.928	43.9	22.9	0.867	0.123	0.112	0.200	0.194	0.056	0.280	1.63
	120	0.007	1.150	0.0488	0.778	43.9	23.1	0.658	0.092	0.084	0.142	0.146	0.030	0.211	1.54
	124	0.007	1.104	0.0620	0.750	43.9	22.4	0.628	0.086	0.079	0.133	0.136	0.019	0.143	1.54
	175	0.010	1.004	0.1560	0.604	43.9	15.9	0.525	0.055	0.048	0.087	0.085	0.014	0.161	1.57
	209	0.012	0.992	0.2020	0.549	43.9	13.3	0.508	0.045	0.038	0.064	0.068	0.019	0.297	1.44
	181	0.010	0.932	0.1830	0.571	43.9	15.3	0.513	0.049	0.043	0.062	0.075	0.025	0.403	1.27
	249	0.014	0.850	0.2840	0.465	43.9	11.2	0.505	0.030	0.025	0.052	0.045	0.002	0.038	1.74
21600	98	0.005	1.359	0.0038	0.938	43.9	28.4	0.885	0.101	0.094	0.180	0.161	0.104	0.578	1.78
	146	0.007	1.166	0.0829	0.711	43.9	19.0	0.592	0.063	0.056	0.094	0.098	0.020	0.213	1.49
	167	0.008	1.049	0.1350	0.631	43.9	16.7	0.537	0.049	0.043	0.059	0.076	0.012	0.203	1.20
	225	0.010	0.950	0.2320	0.517	43.9	12.4	0.503	0.031	0.026	0.042	0.047	0.004	0.095	1.35
	257	0.012	0.939	0.2680	0.481	43.9	10.8	0.503	0.026	0.021	0.031	0.039	0.008	0.258	1.19
	329	0.015	0.832	0.3580	0.400	43.9	8.5	0.522	0.016	0.013	0.023	0.023	0.000	0.000	1.40
28100	103	0.004	1.450	0.0033	0.942	43.9	26.9	0.892	0.078	0.072	0.175	0.125	0.109	0.623	2.24
	166	0.006	1.152	0.1130	0.663	43.9	16.7	0.555	0.042	0.037	0.076	0.065	0.021	0.276	1.81
	194	0.007	1.038	0.1740	0.582	43.9	14.3	0.516	0.032	0.027	0.047	0.048	0.021	0.447	1.48
	326	0.012	0.921	0.3310	0.424	43.9	8.5	0.514	0.015	0.011	0.033	0.021	0.003	0.091	2.26
	332	0.012	0.882	0.3460	0.411	43.9	8.4	0.518	0.014	0.010	0.024	0.019	0.000	0.000	1.78
	292	0.010	0.867	0.3190	0.434	43.9	9.5	0.511	0.016	0.012	0.032	0.023	0.000	0.000	2.06
11100[b])	88	0.008	1.201	0.0045	0.933	43.9	31.8	0.876	0.194	0.182	0.316	0.311	0.053	0.160	1.63
	89	0.008	1.298	0.0013	0.964	33.0	23.6	0.931	0.203	0.186	0.375	0.321	0.060	0.168	1.85
	92	0.008	1.249	0.0052	0.927	10.5	7.2	0.867	0.192	0.139	0.298	0.267	0.074	0.248	1.55
	95	0.009	1.394	0.0014	0.962	21.5	14.3	0.929	0.202	0.174	0.358	0.309	0.083	0.232	1.77
	91	0.008	1.296	0.0026	0.949	58.4	40.6	0.904	0.198	0.189	0.355	0.321	0.054	0.152	1.79
	82	0.007	1.201	0.0015	0.961	23.8	18.3	0.926	0.202	0.180	0.377	0.315	0.061	0.162	1.86
	93	0.008	1.351	0.0014	0.962	83.6	57.3	0.929	0.202	0.195	0.361	0.330	0.065	0.180	1.78
	90	0.008	1.216	0.0051	0.928	38.1	27.0	0.868	0.192	0.178	0.351	0.306	0.052	0.148	1.82

[a]) These data were obtained from Ref. [6] [b]) These data were obtained from Ref. [2] [c]) The ratio $\gamma = M_n(S)/M_n$ of the molecular masses of the short segments along the junction precursor to the long chains. [d]) The volume fraction of the elastically active chains in the dry unswollen state. [e]) Values of the phantom modulus using the usual assumption of a unimodal network, from Eq. (9). [f]) Values of the phantom modulus using the revised Eq. (7), which recognizes the bimodal nature of the network. [g]) Values of the ratio $[f^*]_b/[f^*]_u$ as identified with $2C_1/vRT$.

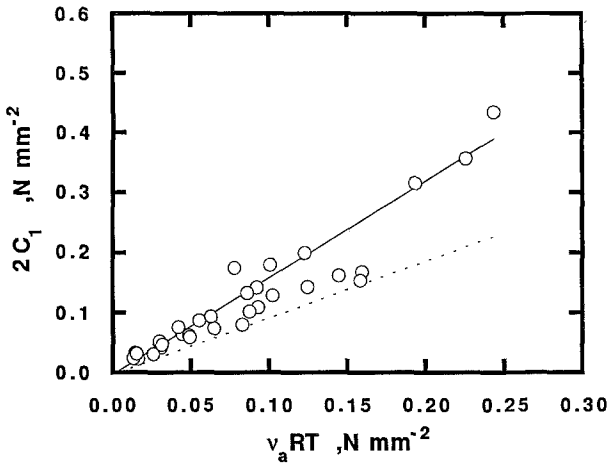

Fig. 2. Experimental values of the high-deformation modulus (approximated by the Mooney–Rivlin constant $2C_1$) compared to the corresponding quantity vRT (where v is the number of network chains obtained from the reaction chemistry). The experimental results, from the work of Kirk et al. [6], are represented by the symbols. The dashed line represents results calculated using the usual assumption that the network is unimodal, i.e., from Eq. (10). The solid line represents calculations based on the revised Eq. (8), which recognizes the bimodal nature of these networks

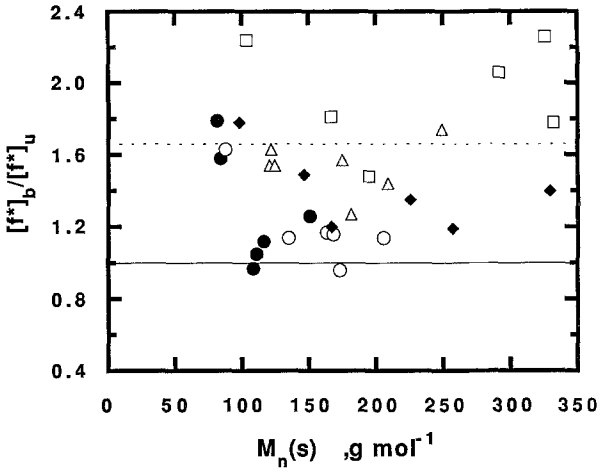

Fig. 3. Values of the ratio $[f^*]_b/[f^*]_u$ as identified with $2C_1/vRT$ as a function of the molecular mass of the short segments M_n(S) (6). The dotted line is the upper asymptote calculated on the assumption that the high-functionality networks are bimodal in both chain length distribution and in functionality, and the solid line is the lower bound, on the assumption that these networks have simple unimodal distributions. The asymptotes were calculated from Eqs. (9) and (10), respectively. The data points are for networks having $M_n = 9320$ (●), $M_n = 1100$ (○), $M_n = 17400$ (△), $M_n = 21600$ (◆), and $M_n = 28100$ (□)

expected [1–7]. Small values of $2C_2$ in this case require that junction fluctuations be suppressed at all elongations by copious chain-junction entangling [9–12]. Relevant here is the fact that the numerous short chains present in these bimodal networks are attached to junctions of functionality three (the smallest possible), and have decreased interpenetration with other network chains because of their shortness [12, 13, 22]. As a result, the suppression of the fluctuations associated with the short chains will be much less than that associated with long chains previously thought to be simply attached to junctions of very high functionality. As discussed elsewhere, the Flory-Erman theory does, in fact, quantitatively predict that this should lead to higher values of $2C_2$ and $2C_2/2C_1$ [12, 13].

In order to characterize the effects of the network long chains, data [6] for the networks having M_n of 9900, 11 100, 17 100, 21 600, and 28 100 g mol^{-1} were analyzed in greater detail. The results are given in Table 1. The above equations suggest that the quantity of primary interest is the ratio $[f^*]_b/[f^*]_u$ of the value of the phantom modulus calculated on the assumption that these networks have a bimodal distribution of crosslink functionalities (Eq. (8)), to that calculated on the assumption that they are unimodal trifunctional ones (Eq. (10)). Figure 3 shows this ratio as identified with $2C_1/vRT$ as a function of the molecular mass M_n(S) of the short segments along the end-linking molecule. Increase in the modulus corresponds to decreasing the lengths of the short chains, which would then increase the effective functionality sensed by the long chains, and increase $[f^*]_b/[f^*]_u$ toward its maximum value of $5/3 = 1.67$. Although the data scatter somewhat, they definitely do show this trend. The transition towards the trifunctional unimodal limit discussed above is seen to occur at M_n(S) of about 100 g mol^{-1}. If the phantom modulus were independent of the chain-length distribution, this ratio should have remained equal to unity (as shown by the solid line). The data obtained at the higher value $M_n = 28\,100$ g mol^{-1} shows considerable scattering, which could be due to associated difficulties in obtaining true equilibrium values of a network having such a low degree of cross-linking [22, 27]. Values of M_n(S) thus

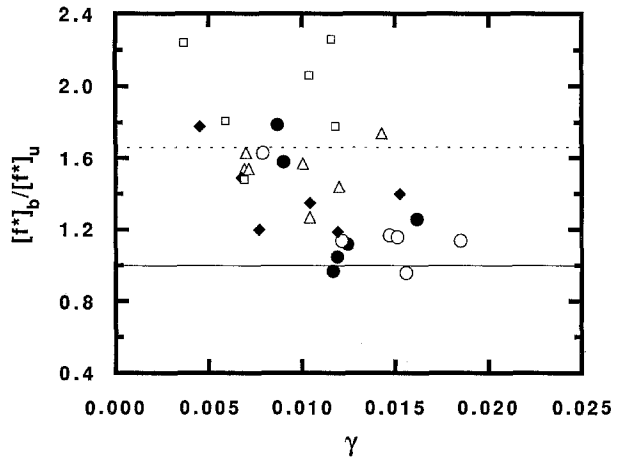

Fig. 4. Values of the ratio $[f^*]_b/[f^*]_u$ as identified by $2C_1/\nu RT$ as a function of the ratio $\gamma = M_n(S)/M_n$ of the molecular masses of the short segments along the junction precursor to the long chains [6]. See legend of Fig. 3

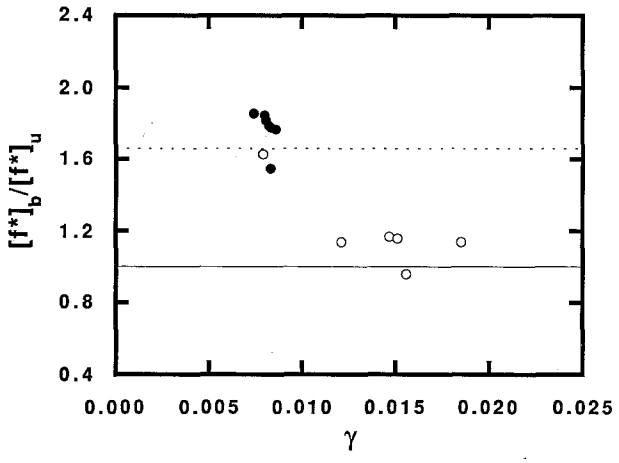

Fig. 5. Values of the ratio $[f^*]_b/[f^*]_u$ as identified with $2C_1/\nu RT$ as a function of $\gamma = M_n(S)/M_n$. The experimental points correspond to two sets of data for networks having $M_n = 11{,}100$ g mol^{-1}. The open circles represent results obtained by Kirk et al. [6], and the filled circles those by Meyers et al. [2], as described in the text

obtained would correspond to short segments having about five bonds. In this regard, it is worth noting that the length of the short chains that was expected to give the maximum enhancement of properties of random bimodal networks was though to be fewer than six bonds [16, 17]. The networks become increasingly monofunctional as the functionality of both the long and short chains approaches three at $M_n(S) = 170$, even though their chain-length distributions are certainly bimodal. The interesting point here is the fact that regardless of the molecular mass M_n of the long chains, the ratio $2C_1/\nu RT$ approaches (5/3) at higher degrees of crosslinking. The transition between the two extremes of (5/3) and 1 is more pronounced at the smaller value of M_n, indicating a strong dependence on M_n, and subsequently on the ratio $M_n(S)/M_n$. The agreement between theory and experiment when such very short chains are considered is seen to be remarkably good.

This phenomenon is explored further in Fig. 4. The ratio $[f^*]_b/[f^*]_u$ is represented as a function of the pertinent ratio $\gamma = M_n(S)/M_n$ of the short chains along the junction precursor to the long ones. Again, the same trends are preserved, with good consistency among all the data points. The bifunctional to monofunctional transition is seen to ensue at a value of $\gamma = 0.007$, with increased monofunctional behavior being approached at a value of 0.015. Even though the values thus obtained seem to be small, it is apparent that all network chains appear to be monofunctional as the functionality approaches three, at least to some extent. This suggests that beyond a certain value of the ratio of chain lengths in a bimodal distribution, the polydispersity of the chain lengths has only a negligible effect on the network's elastomeric properties.

The ratio $[f^*]_b/[f^*]_u$ for the networks having $M_n = 11\,100$ g mol^{-1} is shown plotted against γ in Fig. 5. The data were obtained from two different reports in the literature [2, 6]. The first set of results (shown as filled circles) are for networks that were intentionally prepared so as to have higher extents of reactions, P_{vi} [2]. The resulting values of this ratio are seen to be very close to (5/3) for the networks that inadvertently have low values of $M_n(S)$ (corresponding to higher values of the extent of reaction). The ratio decreases with increase in $M_n(S)$, approaching unity in the limit of low extents of reaction ($P_{vi} \sim 0.40$). As expected, examination of the data [6] analyzed in Table 1 shows that at $P_{vi} > 0.9$, ϕ_L is nearly 35, while at $P_{vi} \approx 0.5$, ϕ_L it is around 11. In other words, the effective value of M_n between cross links increases approximately three-fold as P_{vi} goes from 0.40 to 0.95.

The effects of the extent of reaction are demonstrated further in Fig. 6. The ratio $[f^*]_b/[f^*]_u$ is shown as a function of $\gamma = M_n(S)/M_n$ for

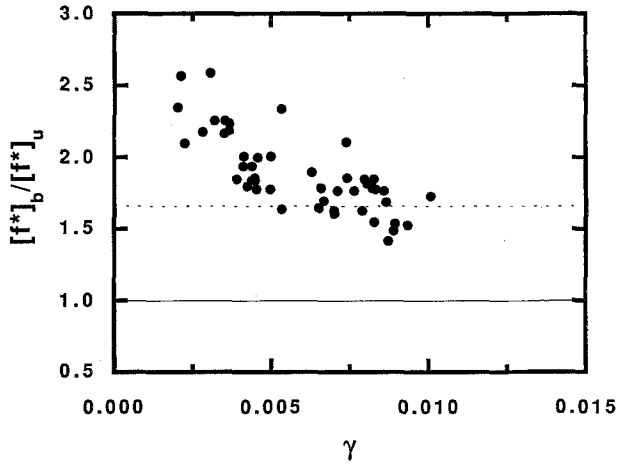

Fig. 6. Values of the ratio $[f^*]_b/[f^*]_u$ as identified with $2C_1/\nu RT$ as a function of $\gamma = M_n(S)/M_n$. The experimental points were obtained by Meyers et al. [2] for high functionality networks intentionally prepared with high extents of reaction, as described in the text

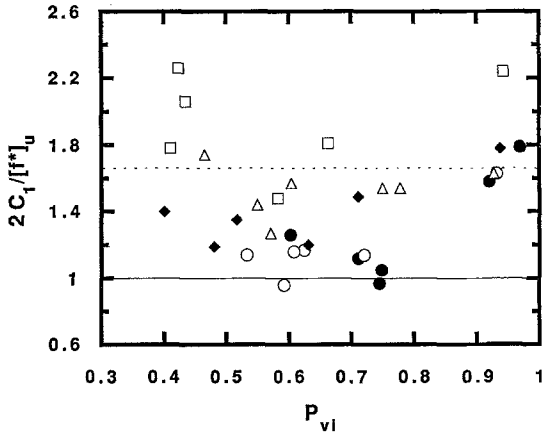

Fig. 7. Values of the ratio $[f^*]_b/[f^*]_u$ as identified with $2C_1/\nu RT$ as a function of the extent of the end-linking reaction. See legend of Fig. 3

networks that were intentionally prepared so as to have high extents of reaction. The data [2] cover a wide range in the degree of cross linking and cross-link functionality. Once again, the ratio is seen to have a value very close to 5/3 for the networks that have low values of $M_n(S)$ (corresponding to higher values of the extent of reaction). In this connection, it is worth noting that the chains coming from the end-linking molecules in such networks would be so short that high elongations could extend them to the extent that the molecules act like "point" junctions of high functionality. Thus far, the results do support the existence of bimodal distributions of cross-link functionalities ($\phi_S = 3$ and $\phi_L > 8$) and chain lengths at relatively small values of the ratio γ.

As would be expected, values of $[f^*]_b/[f^*]_u$ exhibit the same trend when plotted against the extent of reaction P_{vi}, as shown in Fig. 7. This suggests that such behavior can be an important characteristic of elastomeric networks in general. These basic effects are the subject of theories recently developed for regular bimodal networks by Kloczkowski et al. [23] and by Higgs and Ball [24].

The present authors have also interpreted the elastomeric behavior of polysulfidically-cross-linked networks with the methodology used here [14]. In that study, however, changes in the front factor A_ϕ were found to be exactly offset by changes in ν resulting from the counting of the short chains, as the long chains decreased in length. In the present study, however, the two effects are readily separable, because of the much higher values of ϕ. This makes the high-functionality PDMS elastomers particularly important for understanding the dependence of rubber like elasticity on junction functionality and on network chain-length distribution.

In sum, the results thus presented suggest strong dependence of the observed values of the phantom modulus (as identified by $2C_1$) on the network chain-length distribution. Recent theoretical treatments, however, ignore the connectivity of the very short chains to the long ones in order to preserve the cycle rank of the network [23, 24]. At higher values of $M_n(S)$, however, values of $2C_1$ approach those predicted by the network connectivity. In any case, the results clearly elucidate how the effective functionality of the long chains is dependent on the length of the short chains in a bimodal distribution. As such, consideration of the connectivity of the very short chains violates the connectivity requirement of preserving the cycle rank. However, the results are in agreement with our previous assumptions that take into account the connectivity of the very short chains to the long ones in what would essentially be a bimodal network. A preliminary attempt to bridge theory with experiment by one of the authors (EA) is presented in the Appendix.

Appendix

Elastomeric properties of regular bimodal networks at very small values of the ratio of lengths of short and long chains

Kloczkowski, Mark, and Erman (KME) [23] recently developed a molecular theory of junction fluctuations of chain dimensions in regular bimodal networks. In the present investigation, their theory is employed to explain the anomalous elastic behavior (described above) which was observed at very small values of the ratio $\gamma = M_n(S)/M_n$ of the short chains along the junction precursor molecule to the long ones. For this purpose, our starting point will be the unimodal network corresponding to $\gamma = 0$, rather than the regular bimodal network at $0 < \gamma < 1$, as suggested by KME [23]. (We use γ throughout this text instead of ξ used by KME in order to avoid confusion with the cycle rank of the network, usually denoted by ξ). As γ increases, the network becomes increasingly bimodal and presumably again becomes unimodal at $\gamma = 1$. Throughout this transition, it is obvious that the long network chains would sense a decrease in the functionality of the junctions at their ends as γ increased.

The preceding statements will be elaborated upon for networks having high-functionality cross links ($\phi > 8$). Such a network is, in effect, equivalent to an S_2L_1 network, where at each cross-link point along the end-linking molecule, the number of short chains is $\phi_S = 2$ and the number of the long chains is $\phi_L = 1$[12, 13, 29]. Thus, at $\gamma = 0$, the network is undoubtedly unimodal and would presumably have $\phi_L > 8$, as illustrated in part (a) of Fig. 1. As γ increases, the end-linking molecule would act as a sequence of trifunctional junctions with $\phi_L = 1$ and $\phi_S = 2$. Thus the "effective" number of long chains ϕ_L of the long chains changes continuously, and finally becomes unity (presumably at $\gamma = 1$). As illustrated in part (b) of Fig. 1, at very small values of γ, the entire end-linking molecule now acts as one junction of very high functionality. It is to be noted that the junction functionality sensed by short chains is always three. As was described above, there is now a bimodal distribution of cross-link functionality, as well as of network chain length. In order to simplify calculations, we assume a linear dependence of the "effective" number of long chains $\phi_{L,e}$ (emanating from a junction) on γ of the form

$$\phi_{L,e} = \phi_0 - a\gamma \,, \tag{A-1}$$

where ϕ_0 is the functionality of the long chains at $\gamma = 0$, and a is a constant that can be determined from experiment. It is worth mentioning that this expression will result in fractional values of the "effective" functionalities sensed by the long chains, and an increase with increase in γ.

The results presented in Fig. 4 clearly suggest that a transition occurs at very small values of γ (cf. < 0.015) between the bimodal multifunctional limit toward what would appear to be a bimodal trifunctional network. However, such an unusual connectivity of the short chains to the rest of the network at such a small value of γ results in a bimodal distribution of chain lengths. Therefore, at $\gamma = 0.015$, $\phi_{L,e} = 1$ and $\phi_S = 2$. Assuming $\phi_0 = 100$, the value of the constant a obtained in the preceding equation would be 6600. According to the theory of Kloczkowski, Mark, and Erman [23] Eqs. (35-b) and (39) in their model would be expressed as

$$A = \gamma\phi_{L,e}/(\gamma\phi_{L,e} + 2 - \frac{1}{\gamma B} - \gamma B) \tag{A-2}$$

$$\begin{aligned}(\gamma B)^3(\phi_{L,e} - 1) - (\gamma B)^2[(\phi_{L,e} - 3) \\ + \gamma\phi_{L,e}(\phi_{L,e} - 2)] - (\gamma B)[(\phi_{L,e} + 3) \\ + \gamma(\phi_{L,e}^2 + 2\phi_{L,e})] + (\phi_{L,e} + 1) \\ = 0 \qquad\qquad 0 < \gamma \leq 0.015\end{aligned} \tag{A-3}$$

Values of the front factor $A_\phi = (1 - 2/\phi_e)$ (where the "effective" functionality $\phi_e = \phi_{L,e} + \phi_S$) were obtained through iterative calculations based on Eq. (A-3) at different values of γ (employing Eqs. (A-1) and (35-b), (45), (46), and (62) in the model of KME [23]). It has been suggested in the text that the quantity of primary interest is the ratio $[f^*]_b/[f^*]_u$ of the value of the phantom modulus calculated on the assumption that these networks have a bimodal distribution of cross-link functionalities (Eq. (9)), to that calculated on the assumption that they are unimodal trifunctional ones (Eqs. (3) and (5)). Figure A1 shows the effect of γ on this ratio (as given by $(1 - 2/\phi_e)/0.333$, where 0.333 corresponds to the front factor of a unimodal trifunctional network).

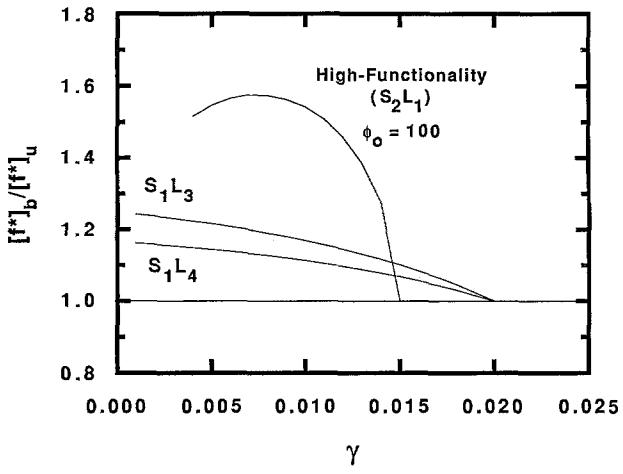

Fig. A-1. Calculated values of the ratio $[f^*]_b/[f^*]_u$ as a function of the ratio $\gamma = M_n(S)/M_n$ of the molecular masses of the short segments along the junction precursor to the long chains. The results were obtained in accordance with the theory of Kloczkowski et al. [23], as described in the Appendix

The results are in qualitative agreement with the experimental results illustrated in Fig. 4, and show an increase in the ratio $[f^*]_b/[f^*]_u$ toward its maximum value of 1.67, at very small values of γ.

Similarly, for the S_1L_3 network, $\phi_{L,e} = 6 - a\gamma$. Assuming that the elastic behavior of a tetrafunctional bimodal network is reached at $\gamma = 0.02$, the value of a so obtained would be 150. Equation (39) in KME [23] will reduce to a second-order equation. Hence, for $S_1L_j (j = 2, 3, \ldots)$ networks, it follows that

$$\gamma B = \{ - [1 - \gamma\phi_{L,e}(\phi_{L,e} - 2)] + \{[1 - \gamma\phi_{L,e}(\phi_{L,e} - 2)]^2 + 4(\phi_{L,e} - 1)(\phi_{L,e} + \gamma\phi_{L,e}^2\}^{1/2}\}/2(\phi_{L,e} - 1) \quad \text{(A-4)}$$

Values of $[f^*]_b/[f^*]_u$ calculated in the same manner approach a maximum of 1.25, as illustrated in Fig. A-1. Such a value is in agreement with experiment [29].A value of 1.2 is obtained for the S_1L_4 network, in agreement with calculations based on structural considerations and the connectivity of the short chains to the long ones. [29].

In the case of the S_1L_2 network, $\phi_S = 1$ and $\phi_L = 2$. At $\gamma = 0$, the "effective" number of the long chains $\phi_{L,e}$ would be expressed by $\phi_{L,e} = 4 - a\gamma$. As γ increases from zero, $\phi_{L,e}$ would change gradually from 4 to 2. There is now growing experimental evidence that the transition for natural rubber networks between the multifunctional bimodal behavior to the trifunctional bimodal limit occurs in the vicinity $\gamma \approx 0.1$ [14]. The results are demonstrated in Fig. A-1. It is noted that the maximum value of $[f^*]_b/[f^*]_u$ calculated is 1.5, as opposed to the value 1.33 predicted on the basis of structural considerations and the connectivity of the short chains to the long ones [14].

It is apparent that when the "effective" functionality of the long chains at very small values of γ is taken into consideration, the results agree with experimental observations, at least qualitatively. However, these calculations are far from rigorous in that the parameter a is little more than an experimental correlation factor. The KME theory has the advantage of being comprehensive and much more molecular in concept.

Acknowledgement

JEM wishes to acknowledge, with gratitude, the financial support provided by the National Science Foundation through Grant DMR 89-18002 (Polymers Program, Division of Materials Research). Our thanks are also extended to Professor A. Khalil and Dr. A. Shalabi for several helpful discussions.

References

1. Lorente MA, Mark JE (1980) Macromolecules 13:681
2. Meyers KO, Bye ML, Merrill EW (1980) Macromolecules 13:1045
3. Gottlieb M, Macoscko CW, Benjamin GS, Meyers KO, Merrill EW (1981) Macromolecules 14:1039, and references cited therein
4. Meyers KO PhD (1980) Thesis in Chemical Engineering, Massachusetts Institute of Technology
5. Meyers KO, Merrill EW In: Mark JE, Lal J (eds) Elastomers and Rubber Elasticity, Am Chem Soc, Washington, DC, 1982
6. Kirk KA, Bidstrup SA, Merrill EW, Meyers KO (1982) Macromolecules 15:1123
7. Opperman W, Rehage G, In: JE Mark and J Lal (eds) Elastomers and Rubber Elasticity, (Am Chem Soc, Washington, DC, 1982)
8. Flory PJ (1977) J Chem Phys 66:5726
9. Flory PJ, Erman B (1982) Macromolecules 15:800
10. Mark JE, Erman B Rubber Elasticity. A Molecular Primer, Wiley Interscience, New York, 1988
11. Flory PJ, Erman B (1984) J Polym Sci, Polym Phys Ed 22:49
12. Sharaf MA, Mark JE (1991) Polym Preprints Am Chem Soc 32 (1):57

13. Sharaf MA, Mark JE (1990) Polym Mat Sci Eng Preprints 62:644; ms. submitted to J Polym Sci Polym Phys Ed
14. Sharaf MA, Mark JE (1991) J Macromol Sci, Macromol Rep A29:67
15. Sharaf MA (1993) J Macromol Sci, Macromol Reports A30:83
16. Llorente MA, Andrady AL, Mark JE (1981) J Polym Sci, Polym Phys Ed 19:623
17. Mark JE, Tang M-Y (1984) J Polym Sci, Polym Phys Ed 22:1849
18. Graessley WW (1975) Macromolecules 8:186
19. Pearson DS, Graessley WW (1978) Macromolecules 11:528
20. Pearson DS, Graessley WW (1980) Macromolecules 13:1001
21. Dossin LM, Graessley WW (1979) Macromolecules 12:123
22. Quesel JP, Mark JE (1985) Adv Polym Sci 71:229
23. Kloczkowski A, Mark JE, Erman B (1991) Macromolecules 24:3266
24. Higgs PG, Ball RC (1989) J Phys (Fr). 49:1785
25. Mooney M (1940) J Appl Phys 11:582
26. Rivilin RS (1948) Philos Trans Roy Soc London, Ser A 241:379
27. Erman B, Flory PJ (1982) Macromolecules 15:806
28. Sharaf MA (1992) Int J Polym Mat 18, 237
29. Sharaf MA, Mark JE, AL Hosani ZY, in press, Eur Polym J

Received May 13, 1993;
accepted September 10, 1993

Authors' addresses:

Professor M.A. Sharaf*, Professor J.E. Mark
Department of Chemistry and Polymer Research Center
The University of Cincinnati,
Cincinnati, OH 45221-0172 USA

Professor E. Ahmed
Department of Mathematics
United Arab Emirates University
P.O. Box 17551, Al Ain
United Arab Emirates